

Benzene chemisorption on palladium surfaces.

I. High-resolution electron-energy-loss vibrational spectra and structural models

G. D. Waddill and L. L. Kesmodel

Department of Physics, Indiana University, Bloomington, Indiana 47405

(Received 30 October 1984)

Benzene chemisorption on Pd(111) and Pd(100) crystal faces at 300 K has been studied by high-resolution electron-energy-loss spectroscopy and thermal desorption spectroscopy. Our results indicate that benzene chemisorbs associatively at only one site and is π bonded with its ring plane parallel to the metal surface. Thermal desorption studies indicate that benzene adsorption is only partially reversible, with decomposition evolving H_2 and leaving a carbon-covered surface as the competing mechanism to benzene thermal desorption. The similarity of the benzene vibrational spectra on Pd(100) and Pd(111) has led us to propose a new model for benzene chemisorption on transition-metal surfaces involving a lower adsorption-site symmetry (C_s) than has been previously suggested.

I. INTRODUCTION

Identification of the conformation and bonding interactions of hydrocarbon molecules on transition-metal surfaces is of fundamental importance in surface science. An understanding of these quantities could provide useful insight into the processes occurring during catalyzed surface reactions. By employing high-resolution electron-energy-loss spectroscopy (HREELS) and thermal desorption spectroscopy (TDS), the identification and understanding of these quantities is possible.

This paper presents a detailed study of room-temperature benzene adsorption on the (111) and (100) crystal faces of palladium. An attempt to determine the molecular-adsorption geometry and site symmetry is made by use of the surface-dipole-selection rule in conjunction with angle-dependent HREELS data. Previous results on other transition-metal surfaces have determined that benzene chemisorbs associatively with its ring plane parallel to the surface, bonding being through π orbitals.¹⁻⁴ Studies of benzene adsorption on Pt(111),^{3,5} Pt[6(111)×(111)],⁵ Ni(111),³ and Rh(111) (Ref. 4) crystal faces suggest the existence of two differentiable benzene-chemisorption sites on these surfaces.

Our study suggests the presence of only one benzene-chemisorption site on the Pd surfaces investigated. Furthermore, the striking similarity of the HREELS spectra on Pd(100) and Pd(111), combined with the angle-dependent scattering data, has led us to a new model for benzene chemisorption on transition-metal surfaces which involves lower site symmetry (C_s) than previously suggested. This model removes several inconsistencies of earlier mode assignments and leads to a unified picture of benzene adsorption on (100) and (111) surfaces involving bridge-bonding sites.

In the present paper we focus on interpretation of the benzene vibrational spectra and the problem of site-symmetry determination. In a subsequent paper we shall discuss the beam-energy dependence of the HREELS

spectra, which recently provided strong evidence of negative-ion resonance scattering on the Pd(100) surface.⁶

II. EXPERIMENTAL

The experiments were performed in two ultrahigh-vacuum chambers at Indiana University. The Pd(111) experiments were carried out in an ion- and sublimation-pumped chamber (base pressure $\sim 1 \times 10^{-10}$ Torr) equipped with HREELS, ion-sputtering, and mass spectrometry. The HREELS measurements were made with a single-pass 127° cylindrical deflection electron spectrometer⁷ operated at 7.5-meV (60-cm^{-1}) resolution with typical elastic beam rates of $(7-8) \times 10^4$ cps for benzene adsorption. Thermal-desorption measurements were performed with a quadrupole mass spectrometer (Uthe Technology International, Model 100C) which was externally driven to allow for rapid scanning and recording of ion current for different atomic mass units. A stainless-steel tube was extended from the mass spectrometer ionizer to the center of the vacuum chamber. The spectra were recorded with the crystal ~ 5 mm from the tube opening and facing it. Contributions to the ion current due to desorption from the chamber walls, manipulator arms, etc., were determined to be negligible by performing identical experiments with the crystal face rotated 90° away from the tube opening. The heating rate was typically 1 K/sec and was linear over the temperature range investigated.

The Pd(100) experiments were performed in a diffusion- and sublimation-pumped chamber (base pressure $\sim 5 \times 10^{-11}$ Torr) equipped for ion-sputtering, low-energy electron diffraction, Auger spectroscopy, and HREELS. The HREELS measurements were made with a double-pass 127° cylindrical deflection electron spectrometer⁸ also operated at 7.5-meV (60-cm^{-1}) resolution, but with elastic beam rates of $\sim 2 \times 10^6$ cps for benzene adsorption.

Sample preparation and cleaning have been described

elsewhere.⁹ High-purity C_6H_6 and C_6D_6 were used, their purity being monitored with the mass spectrometer. Exposures quoted in langmuirs ($1 L = 10^{-6}$ Torr sec) have been corrected for ion-gauge sensitivity.¹⁰

III. RESULTS

A. Pd(111) Thermal desorption

Heating of the $C_6H_6/Pd(111)$ surface leads to competing benzene thermal desorption and decomposition reactions. Similar results have been obtained for benzene adsorption on Ni,¹¹ Pt,^{5,12} and Rh.⁴ Figures 1 and 2 show the thermal desorption spectra for C_6H_6 and H_2 , respectively, following exposure of the Pd(111) surface to C_6H_6 at 300 K. For benzene exposures less than 0.5 L, there is no detectable molecular C_6H_6 thermal desorption, only dehydrogenation yielding H_2 desorption and surface carbon. Some reversible benzene chemisorption occurs for exposures ≥ 0.5 L. At 0.5-L exposure, there is one benzene thermal desorption peak at 550 K which shifts gradually to its saturation coverage ($\sim 1L$) value of ~ 525 K upon increasing initial benzene coverage. In addition, a second C_6H_6 desorption peak appears at ~ 430 K as the initial benzene coverage is increased. The intensity ratio of the two peaks is $\sim 1:1$ at saturation coverage.

Benzene dehydrogenation always occurs following benzene thermal desorption. For irreversible benzene coverages (< 0.5 L), H_2 desorption occurs at ~ 560 K. This peak shifts to ~ 540 K with the onset of reversible benzene chemisorption.

Similar thermal desorption behavior was observed for $C_6D_6/Pd(111)$ with both C_6D_6 -desorption peaks and the one D_2 -desorption peak occurring ~ 15 K higher than their corresponding C_6H_6 - and H_2 -desorption peaks. The deuterated spectra exhibit the same initial exposure dependence as the nondeuterated spectra. Co-adsorption of C_6H_6 and C_6D_6 yielded all possible $C_6H_xD_{6-x}$ molecules in the high-temperature peak. The amount of exchange, however, was low ($< 20\%$). In addition, H_2 , HD, and D_2 peaks were all observed in the temperature region characteristic of benzene dehydrogenation.

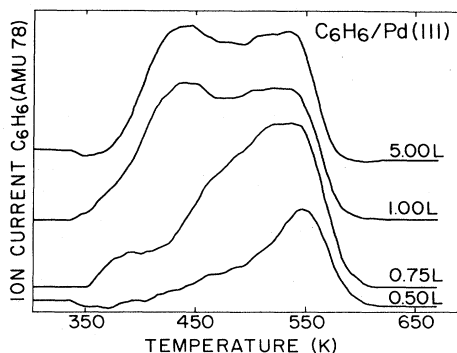


FIG. 1. Thermal desorption spectra for C_6H_6 chemisorbed on Pd(111) at 300 K as a function of initial surface coverage.

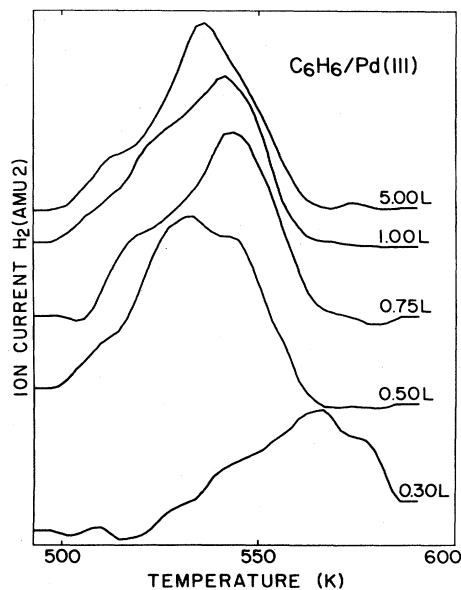


FIG. 2. Thermal desorption spectra of H_2 following C_6H_6 chemisorption on Pd(111) at 300 K as a function of initial surface coverage.

B. High-resolution electron-energy-loss spectroscopy

Room-temperature adsorption of C_6H_6 on Pd(111) and Pd(100) yields almost identical spectra for both surfaces over the exposure range investigated (0.1–5.0 L). There were no exposure dependencies in the spectra other than an overall increase in the vibrational-loss intensities with increasing initial exposure. Our vibrational spectra for benzene adsorption on Pd(111) and Pd(100) are remarkably similar to benzene vibrational spectra on a number of other transition-metal surfaces. These spectra have been consistently interpreted as indicating that benzene adsorbs with its ring plane parallel to the metal surface, bonding being through π orbitals.^{1–4} Specular and off-specular data have been extensively investigated to facilitate mode assignments. The off-specular data were obtained by rotating the sample through the appropriate angle. The energy dependence of the modes was also investigated but will not be discussed here.^{6,13}

Representative spectra for specular and 6° off-specular scattering from $C_6H_6/Pd(111)$ are shown in Fig. 3. Figure 4 shows the same spectra for scattering from $C_6D_6/Pd(111)$. Analogous spectra for Pd(100) are shown in Figs. 5 and 6. The vibrational frequencies are given in Table I along with the dominant scattering mechanism and the mode number and representation for the corresponding gas- (or liquid-) phase frequencies. The dominant scattering mechanism is determined from the behavior of vibrational-loss intensity as a function of angle off-specular. Here vibrational modes which are dipole-enhanced exhibit a strong specular lobe of narrow angular width,¹⁴ while modes which exhibit broad angular behavior are attributed to a short-range impact scattering mechanism. On Pd(111), moving from specular to 6° off-

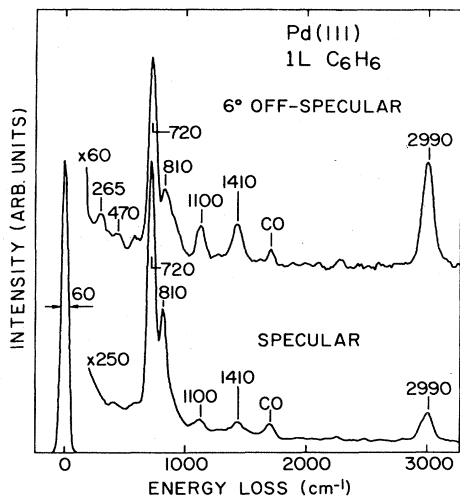


FIG. 3. Comparison of the high-resolution electron-energy-loss spectra for 300-K adsorption of C_6H_6 on Pd(111) for specular and 6° off-specular scattering. Incident-beam energy was 2.5 eV.

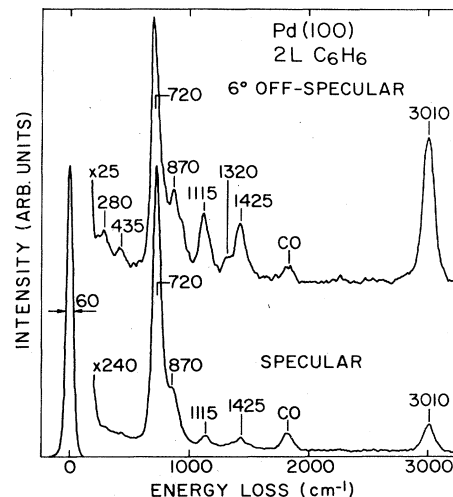


FIG. 5. Comparison of the high-resolution electron-energy-loss spectra for 300-K adsorption of C_6H_6 on Pd(100) for specular and 6° off-specular scattering. Incident-beam energy was 2.7 eV.

specular scattering decreases the intensities of the losses at 1100, 1410, and 2990 cm^{-1} by factors of ~ 1.3 – 1.7 (implying predominantly impact scattering), while it decreases the intensities of the losses at 720 and 810 cm^{-1} by a factor of ~ 6 (predominantly dipole scattering). The elastic peak intensity decreases by a factor of ~ 15 . On Pd(100) the intensities of the losses at 1115, 1320, 1425, and 3010 cm^{-1} decrease by factors of ~ 1.0 – 1.5 , while the intensities of the 720- and 870-cm^{-1} losses decrease by factors of ~ 10 – 20 on moving from specular to 6° off-specular scattering. On Pd(100) the elastic peak intensity decreases by a factor of ~ 50 on moving to 6° off-specular

scattering. Despite the importance of impact scattering from a large number of the vibrational modes, there is also a dipole scattering contributions to all the losses.

Isotopic shifts of the 720-, 810-, 1100-, and 2990-cm^{-1} losses for Pd(111) and of the 720-, 870-, 1115-, and 3010-cm^{-1} losses for Pd(100) establish these as C-H vibrations. Comparison with gas-phase frequency values of 673, 1150, and 3062 cm^{-1} implies that the losses at 720, ~ 1100 , and 3000 cm^{-1} be assigned to ν_4 , ν_{10} , and ν_1 , respectively. The C-H vibrational loss at $\sim 800\text{ cm}^{-1}$ will

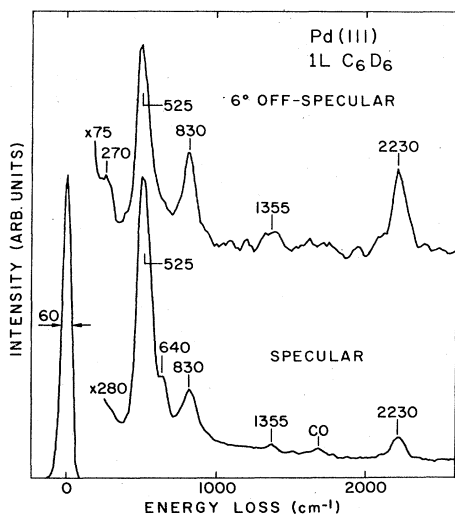


FIG. 4. Comparison of the high-resolution electron-energy-loss spectra for 300-K adsorption of C_6D_6 on Pd(111) for specular and 6° off-specular scattering. Incident-beam energy was 2.5 eV.

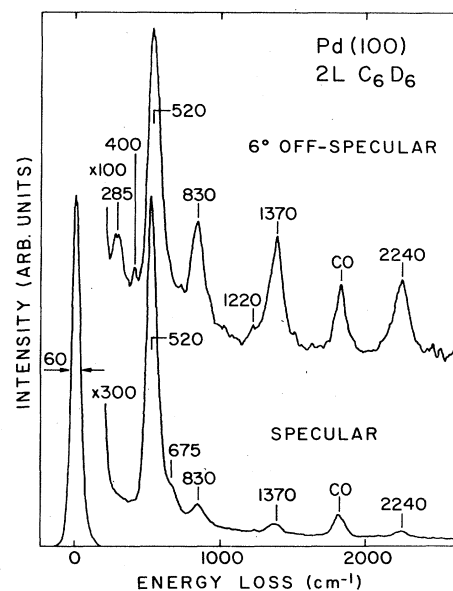


FIG. 6. Comparison of the high-resolution electron-energy-loss spectra for 300-K adsorption of C_6D_6 on Pd(100) for specular and 6° off-specular scattering. Incident-beam energy was 4.6 eV.

TABLE I. Assignment of the observed vibrational frequencies (cm^{-1}) for benzene chemisorbed on Pd(111) and Pd(100) at 300 K.

Chemisorbed frequencies		Gas- or liquid-phase frequencies ^a	Mode No. and rep.	Mode	Dominant mechanism
Pd(111) C_6H_6 (C_6D_6)	Pd(100) C_6H_6 (C_6D_6)				
265 (270)	280 (285)			$\nu_{\text{Pd-C}}$	Dipole
470 (not obs.) ^b	435 (400) ^b	c	b	$\nu_{\text{Pd-C}}^{\text{b}}$	Dipole
720 (525)	720 (520)	673 (497)	ν_4 (A_{2u})	γ_{CH}	Dipole
810 (640)	870 (675)	849 (662)	ν_{11} (E_{1g})	γ_{CH}	Dipole
not obs. (830)	not obs. (830)	992 (943)	ν_2 (A_{1g})	ν_{CH}	Not determined
1100 (830)	1115 (830)	1150 (824)	ν_{10} (B_{2u})	δ_{CH}	Impact
not obs.	1320 (1220)	1310 (1286)	ν_9 (B_{2u})	ν_{CC}	Impact
1410 (1355)	1425 (1370)	1486 (1335)	ν_{13} (E_{1u})	δ_{CC}	Impact
2990 (2230)	3010 (2240)	3062 (2293)	ν_1 (A_{1g})	ν_{CH}	Impact

^aReference 16.

^bAlternatively assigned to ν_{20} (ring deform).

^cGas-phase frequencies for ν_{20} are 410 (352) cm^{-1} .

be discussed shortly. On the Pd(100) surface, two C-C vibrational modes are identified at 1320 and 1425 cm^{-1} . The presence of C-C gas-phase modes at 1310 and 1486 cm^{-1} leads us to assign the losses at 1320 and 1425 cm^{-1} to ν_9 and ν_{13} , respectively. Lehwald *et al.*³ did not observe the 1320 - cm^{-1} loss and assigned peaks at 1420 cm^{-1} on Pt(111) and 1430 cm^{-1} on Ni(111) to ν_9 . A later force-field calculation by Jobic *et al.*,¹⁵ however, tends to rule against such a large frequency upshift (gas-phase frequency 1310 cm^{-1}) for ν_9 on adsorption, thus favoring the present assignment. The lower signal levels for the Pd(111) system made identification of the weak ν_9 mode impossible here. The ν_{13} mode, however, was observed at 1410 cm^{-1} . In addition to the C-H and C-C vibrational losses, two Pd-C vibrations are identified at 265 and 470 cm^{-1} for Pd(111) and at 280 and 435 cm^{-1} for Pd(100). The proximity of the 470 - cm^{-1} Pd-C vibration on Pd(111) to the ν_4 mode at 525 cm^{-1} for C_6D_6 adsorption rendered it unobservable in Fig. 4.

The mode at 830 cm^{-1} in the deuterated spectra on both surfaces is believed to be too intense (and also exhibits substantially stronger dipole activity than the corresponding mode of approximately 1100 cm^{-1}) to be exclusively due to the ν_{10} C-D bending mode, and has been additionally assigned to the ν_2 ring-stretching mode. This is consistent with mode assignments for $\text{C}_6\text{H}_6/\text{Rh}(111)$.⁴ The ν_2 contribution to this loss is obscured in the nondeuterated spectra by the presence of the strong loss at 810 cm^{-1} on Pd(111) and 870 cm^{-1} on Pd(100). This loss has been assigned to the ν_{11} mode. The assignment of this loss to ν_{11} is predicated upon the observation of a strong ν_{11} C-H vibration at 849 cm^{-1} in the liquid phase.¹⁶ While this mode is not infrared-active in the liquid phase, it is an out-of-plane C-H bending mode that would likely become dipole-active given the proper adsorption-site symmetry. The assignment of this loss to ν_{11} is also in agreement with assignments by Jobic *et al.*¹⁵ on Raney Ni, and by Moskovits and DiLella on Ag.¹⁷ It should be mentioned that on a number of transition-metal surfaces, the two strong losses in the region 700 – 950 cm^{-1} have been interpreted as both being ν_4 modes corresponding to different benzene-adsorption sites. Support for this inter-

pretation is given by the wide variation of the intensity ratio of the two peaks with coverage and temperature. This, however, was not found to be the case on the Pd surfaces investigated here. The I_{720}/I_{810} ratio remains constant at $\sim 2/1$ over the entire exposure (0.1 – 5.0 L) and temperature range [150 – 500 K for Pd(111)] investigated. The same was found to be true on the Pd(100) surface (exposure range 0.1 – 5.0 L, temperature range 300 – 500 K) with the intensity ratio I_{720}/I_{870} being $\sim 5/1$.

These spectra, along with the TDS data, establish that benzene is molecularly chemisorbed and, on the basis of small shifts from gas-phase vibrational frequencies upon chemisorption, undergoes no substantial rehybridization. The strong intensity of the ν_4 out-of-plane C-H bending mode along with the relatively weak intensity of the ν_1 planar C-H stretching mode in the spectra indicate that benzene adsorbs with its ring plane parallel to the metal surface. In gas-phase infrared spectra, modes having dynamic dipole moments parallel to the ring plane ($\nu_{12}, \nu_{13}, \nu_{14}$) and modes having dynamic dipole moments perpendicular to the ring plane (ν_4) have similar intensities. The strong intensity of the ν_4 mode and the weak intensity of the in-plane ν_1 C-H stretching mode is due to the arrangement of benzene with its ring plane parallel to the surface and the conditions of the surface dipole selection rule.¹⁸ This rule states that only vibrational modes with dynamic dipole moments perpendicular to the surface will be observed as dipole active modes.

IV. DISCUSSION

A. Pd(111) TDS

The properties of the benzene thermal-desorption spectra can be explained by (i) the existence of two benzene chemisorption states with different desorption energies or (ii) repulsive interactions between benzene molecules at high coverages. The following results give strong evidence that the latter is responsible for the observed spectra.

(i) The Pd(111) crystal surface was exposed to 0.3 L C_6D_6 , and then further exposed to 2.0 L C_6H_6 . The re-

sulting spectra not only showed C_6D_6 desorption, which would not normally be observed for such a low initial C_6D_6 exposure, but also showed no difference in the $I_{C_6H_6}/I_{C_6D_6}$ intensity ratio for both desorption peaks.

(ii) The Pd(111) crystal surface was exposed to 0.5 L C_6D_6 , and then further exposed to 2.0 L C_6H_6 . Normally such an initial exposure of C_6D_6 would result in observation of only the high-temperature benzene desorption peak; however, the observed spectra yielded both desorption peaks for C_6D_6 and C_6H_6 . Again, there was no difference in the $I_{C_6H_6}/I_{C_6D_6}$ ratio for both of these peaks.

(iii) The Pd(111) crystal surface was exposed to 2.0 L C_6D_6 and then further exposed to 2.0 L C_6H_6 . The resulting spectra indicate that most of the C_6D_6 was displaced by C_6H_6 .

While these results do not exclude the possibility of rapid migration between two benzene-adsorption sites, they strongly suggest that the existence of two benzene thermal-desorption peaks at high coverages is due to repulsive adsorbate interactions.¹⁹ Similar results for benzene adsorption on the low-Miller-index planes of Pd have been reported previously.²⁰

B. HREELS

One of the most striking features of our results is the similarity of the vibrational spectra of benzene on both Pd-crystal surfaces. Indeed, our spectra are also very similar to vibrational spectra of benzene on a number of other low-Miller-index transition-metal surfaces.¹⁻⁴ This similarity indicates that for benzene chemisorption, either vibrational spectroscopy is not sensitive to the adsorption site, or that the adsorption site is quite similar on all surfaces.

These observations have led us to reexamine previous mode assignments and adsorption site-symmetry determinations on transition-metal surfaces. One major difference between earlier assignments and our assignments lies in the identification of the higher frequency mode of the two relatively strong losses in the region 700–950 cm^{-1} . As previously mentioned, coverage and thermal dependencies of the relative intensities of these two peaks led to the assignment of both to the ν_4 mode. The two ν_4 modes

were attributed to different orientations of the benzene ring with respect to the symmetry planes at the adsorption site.³ For the Pd surfaces we investigated, no coverage or thermal dependencies of the relative intensities of these two peaks was found. Further evidence that these two peaks should not both be assigned to ν_4 is shown in Table II. Here we show vibrational frequencies and isotope shifts for the major C-H vibrational losses on a number of different surfaces. We note here the distinct, systematic difference in deuteration shifts of the ν_4 and ν_{11} (our assignment) modes, and their agreement with gas-phase deuteration shifts, on all the metal surfaces listed. This again places in question the interpretation of these two modes as both being ν_4 losses.

A further important discrepancy in mode assignments lies in the identification of modes in the region 1300–1500 cm^{-1} . We have assigned modes at 1320 and 1425 cm^{-1} on Pd(100) as being ν_9 and ν_{13} , respectively. Lehwald *et al.*³ assigned modes of approximately 1400 cm^{-1} on Pt(111) and Ni(111) to ν_9 , and observed no mode of approximately 1300 cm^{-1} . As mentioned earlier, this assignment requires a large upward frequency shift from the gas-phase value (1310 cm^{-1}), contrary both to valence force-field calculations¹⁵ and vibrational frequencies of complexed benzenes.^{21,22} Disagreement between our assignments and Bertolini's² in this region stem from his questionable assignment of a mode at 1110 (820) cm^{-1} on Ni(111) and Ni(100) to ν_{17} or ν_{19} . (Here and throughout the remainder of the paper, frequencies listed in parentheses refer to C_6D_6 vibrational modes.) We would assign this loss to ν_{10} with the added note that extra intensity for this loss in the deuterated spectra is due to an underlying ν_2 mode as we discussed earlier.

The above considerations have an important bearing on a consistent determination of the adsorption site symmetry for benzene on these surfaces, as will now be discussed. Comparison of the observed modes with those predicted to be dipole-active for the subgroups of D_{6h} allows the determination of the adsorption site symmetry. According to the dipole selection rule¹⁸ only vibrations belonging to the totally symmetric representations A , A' , and A_1 will be observed in dipole scattering. Our selection of adsorption site symmetry is then governed by our assignment of dipole-active losses to the ν_{11} and ν_{13} modes.

TABLE II. A comparison of the vibrational frequencies (cm^{-1}) and deuteration ratios for some benzene C-H vibrations on different single-crystal metal surfaces. The values in parentheses are the corresponding C-D vibrational frequencies.

Crystal surface	ν_4^a	ν_H/ν_D	ν_{11}^a	ν_H/ν_D	ν_{10}^a	ν_H/ν_D	ν_1^a	ν_H/ν_D	Ref.
Ni(111)	745 (540)	1.38	845 (645)	1.31	1110 (820)	1.35	3020 (2290)	1.34	2
Pd(111)	720 (525)	1.37	810 (640)	1.27	1100 (830)	1.33	2990 (2230)	1.34	This work
Pt(111)	830 (610)	1.36	920 (700)	1.31	1130 (800)	1.41	3000 (2240)	1.34	3
Rh(111)	810 (565)	1.43	not obs.		1130 (835)	1.35	3000 (2250)	1.33	4
Ni(100)	750 (540)	1.39	845 (645)	1.31	1120 (820)	1.37	3025 (2260)	1.34	2
Pd(100)	720 (520)	1.38	870 (675)	1.29	1115 (830)	1.34	3010 (2240)	1.34	This work
Gas phase	673 (497)	1.35	849 (662)	1.28	1150 (824)	1.40	3062 (2293)	1.34	16

^aDenotes our mode assignment.

TABLE III. A comparison of the predicted dipole-active modes of benzene and their gas-phase frequencies (cm^{-1}) in the C_s subgroups of D_{6h} and the observed frequencies on Pd(100).

D_{6h} rep. and mode no.	$C_s(\sigma_v)$	$C_s(\sigma_d)$	Dipole activity	Pd(100) observed
A_{1g}	ν_1	3062	a	3010
	ν_2	992	a	b
A_{1u}				
A_{2g}				
A_{2u}	ν_4	673	a	720
B_{1u}	ν_5	3048		
	ν_6	1010		
B_{2g}	ν_7	991		
	ν_8	707		
B_{2u}	ν_9			1320
	ν_{10}			1115
E_{1g}	ν_{11}	849	a	870
E_{1u}	ν_{12}	3057		
	ν_{13}	1486	a	1425
	ν_{14}	1035	a	
	ν_{15}	3047		
E_{2g}	ν_{16}	1595		
	ν_{17}	1177		
	ν_{18}	607		
	ν_{19}	969		
E_{2u}	ν_{19}	969		
	ν_{20}	404		

^aDenotes infrared-active fundamentals in $\text{Cr}(\text{C}_6\text{H}_6)_2$ (Ref. 21).

^bThe position of this mode in nondeuterated spectra cannot be resolved due to overlap with the ν_{11} mode.

While the dominant scattering mechanism for the ν_{13} mode was determined to be impact scattering, we find a significant dipole-scattering contribution (20–40%). For the ν_{11} mode there can be no doubt as to the dominant scattering mechanism being dipole scattering. Examination of the correlation table for point group D_{6h} shows that *neither of these modes should be dipole-active except for the two C_s subgroups*. Thus strict adherence to the dipole selection rule leads us to choose between $C_s(\sigma_v)$ and $C_s(\sigma_d)$ as the highest adsorption site symmetry for these surfaces. In Table III we have tabulated the predicted dipole-active modes for these two subgroups of D_{6h} , along with the observed modes on Pd(100) and the dipole activity of the modes in $\text{Cr}(\text{C}_6\text{H}_6)_2$.²¹ In view of the differences between $C_s(\sigma_v)$ and $C_s(\sigma_d)$ in predicting the activity of the ν_9 and ν_{10} modes, we prefer $C_s(\sigma_d)$ for the adsorption site symmetry on these surfaces. Such a site has its only symmetry plane bisecting C-C bonds in the benzene ring.

While the $C_s(\sigma_d)$ adsorption site symmetry does predict the ν_{11} and ν_{13} modes to be dipole active, it has the drawback of predicting several “unobserved” dipole-active modes. This point deserves further elaboration. All of the predicted but unseen dipole active modes belong to the representations E_{1u} , E_{2g} , and E_{2u} of the point group D_{6h} . Of these modes, only those belonging to the E_{2u} representation are out-of-plane vibrational modes. Thus, it is not too surprising that modes belonging to the E_{1u} and E_{2g} representation, with the exception of ν_{13} , are not seen. We attribute their absence to (i) low dipole activity due to the planar nature of their motions and/or (ii) proximity to a stronger mode which obscures these modes. Two modes,

ν_{19} and ν_{20} , belong to the E_{2u} representation. The ν_{19} mode has a gas-phase frequency of 969 (793 cm^{-1}), and so it may be obscured by the loss of approximately 850 cm^{-1} . Finally, the ν_{20} mode has a gas-phase frequency of $404 (352 \text{ cm}^{-1})$, and could thus be responsible for the loss of approximately 400 cm^{-1} which we alternatively assign to a carbon-metal mode.

In summary, upon noting the similarity in benzene vibrational spectra on a number of transition-metal surfaces, we are led to a reexamination of mode assignments and adsorption-site-symmetry determinations for benzene chemisorption on these surfaces. Our assignment of loss peaks to the ν_{11} and ν_{13} modes, together with strict adherence to the dipole selection rule leads us to determine $C_s(\sigma_d)$ as the adsorption site symmetry for benzene on these surfaces at variance to earlier models which postulated rather high symmetry configurations.

The above arguments are based on adherence to the dipole selection rule for the dipole-active modes. One may argue that this rule does not strictly apply for chemisorbed benzene, in which case detailed site-symmetry arguments based on dipole activity are, of course, invalidated. This point of view was discussed earlier by Bertolini *et al.*² It is our intention to investigate the consequences of adherence to the surface-dipole-selection rule for C_6H_6 adsorption on Pd in light of the suitability of this rule in a number of other investigations.¹⁸

V. CONCLUSIONS

HREELS together with TDS establish that benzene is associatively chemisorbed with its ring plane parallel to

the Pd(111) and Pd(100) surfaces at 300 K. TDS data, along with HREELS results, imply that benzene occupies only one adsorption site on these palladium crystal faces. HREELS data for a number of different surfaces¹⁻⁴ indicate either that benzene vibrational spectra are insensitive to adsorption site, or that the adsorption site is basically the same for all of the surfaces investigated. Strict adherence to the dipole selection rule leads us to postulate an adsorption site on these surfaces of $C_s(\sigma_d)$ symmetry. A bridging site with the benzene between two Pd atoms on the (111) crystal surface is consistent with C_s symmetry provided that metal layers deeper than the first are also

taken into account. On the (100) surface bridge sites are available, but in order to have C_s symmetry, the benzene molecule cannot be centered precisely at the bridge position. Nevertheless, the similarity in the C_s bridging sites on the two surfaces provides further impetus for this model.

ACKNOWLEDGMENTS

We thank Mr. M. K. Hosek and Mr. A. B. Ahmad for expert technical assistance. This work was supported by the Office of Naval Research.

-
- ¹J. C. Bertolini, G. Dalmai-Imelik, and J. Rousseau, *Surf. Sci.* **67**, 478 (1977).
²J. C. Bertolini and J. Rousseau, *Surf. Sci.* **89**, 467 (1979).
³S. Lehwald, H. Ibach, and J. E. Demuth, *Surf. Sci.* **78**, 577 (1978).
⁴B. E. Koel, J. E. Crowell, C. M. Mate, and G. A. Somorjai, *J. Phys. Chem.* **88**, 1988 (1984).
⁵Min-Chi Tsai and E. L. Muettterties, *J. Am. Chem. Soc.* **104**, 2534 (1982).
⁶L. L. Kesmodel, *Phys. Rev. Lett.* **53**, 1001 (1984).
⁷L. L. Kesmodel, J. A. Gates, and Y. W. Chung, *Phys. Rev. B* **23**, 489 (1981).
⁸L. L. Kesmodel, *J. Vac. Sci. Technol.* **A1**, 1456 (1983).
⁹J. A. Gates and L. L. Kesmodel, *Surf. Sci.* **111**, L747 (1981).
¹⁰Varian ionization gauge factor for benzene: 6.0.
¹¹C. M. Friend and E. L. Muettterties, *J. Am. Chem. Soc.* **103**, 773 (1981).
¹²Min-Chi Tsai and E. L. Muettterties, *J. Phys. Chem.* **86**, 5067 (1982).
¹³G. D. Waddill and L. L. Kesmodel (unpublished).
¹⁴E. Evans and D. L. Mills, *Phys. Rev. B* **5**, 4126 (1972); *Surf. Sci.* **48**, 59 (1975).
¹⁵H. Jobic, J. Tomkinson, J. P. Candy, P. Fouilloux, and A. J. Renouprez, *Surf. Sci.* **95**, 496 (1980).
¹⁶L. M. Sverdlov, M. A. Kovner, and E. P. Krainov, *Vibrational Spectra of Polyatomic Molecules* (Wiley, New York, 1974), p. 324.
¹⁷M. Moskovits and D. P. DiLella, *J. Chem. Phys.* **73**, 6068 (1980).
¹⁸See, for example, H. Ibach and D. L. Mills, *Electron Energy Loss Spectroscopy and Surface Vibrations* (Academic, New York, 1982).
¹⁹For the consequences of repulsive adsorbate interactions on TDS see, for example, D. L. Adams, *Surf. Sci.* **42**, 12 (1974).
²⁰T. M. Gentle and E. L. Muettterties, *J. Phys. Chem.* **87**, 2469 (1983).
²¹R. G. Snyder, *Spectrochim. Acta* **10**, 807 (1959).
²²I. J. Hyams and E. R. Lippincott, *Spectrochim. Acta* **28A**, 1741 (1972).